

Aerodynamic Measurements About a Rotating Propeller with a Laser Velocimeter

J Lepicovsky* and W A Bell†
Lockheed-Georgia Company, Marietta, Georgia

The objective of this work was to develop and verify a data acquisition and reduction conditional sampling technique suitable for the laser velocimeter which would allow multicomponent velocity and turbulence intensity measurements near and between the rotating propeller or fan blades. A relatively simple experiment was set up to measure the flowfield of a two bladed propeller operating at static (nonflight) conditions to verify these procedures. The program consisted of acquiring time averaged, mean and ensemble averaged, blade to blade distributions of velocity and turbulence intensity data for all three velocity components. Separated and reverse flow regions were located on a rotating static propeller. The radial distribution of the static propeller section angle of attack was also measured during rotation. Blade to blade distributions revealed that a negative prewhirl exists in front of the propeller disk. Behind the propeller, a distinct distortion of the flowfield due to the presence of the propeller blade wake was observed.

Nomenclature

D	= propeller tip diameter
i	= local turbulence intensity
i	= angle of attack
I	= mean turbulence intensity
M	= Mach number
n	= number of revolutions
R	= propeller tip radius ($R = D/2$)
U	= circumferential velocity
V	= absolute flow velocity
W	= relative flow velocity
X, Y, Z	= coordinates
α	= absolute flow angle
β	= relative flow angle
Δv	= local velocity amplitude
θ	= blade angular position
ϕ	= blade pitch angle

Subscripts

A	= axial
BT	= blade tip
R	= radial
T	= tangential

Introduction

THE flow through an aircraft propeller or helicopter rotor is a very complex three dimensional flowfield involving wake/freestream interaction and wake decay vortex shedding tip vortex/wake interaction and viscous flow separation. The phenomena are often accompanied by intensive local backflows in the flowfield about a hovering propeller or rotor or a propeller at very low flight velocity.

The experimental techniques currently used in propeller aerodynamic research are often unable to completely measure the fine details of the nonstationary velocity flowfield of a rotating propeller or rotor. The restrictions of the conventional experimental techniques are dictated by either

inherently low probe natural frequency or low directional sensitivity and directional ambiguity. In some cases, the probe can also be affected by flow parameters other than the velocity. The major drawback, however, is that a solid probe has to be immersed into the flow. The probe interacts with a flowfield of a rotating propeller or rotor and may distort the measured velocity flow pattern.

The laser velocimeter (LV) a nonintrusive measuring instrument can overcome some of these problems. Attempts to use the laser velocimeter for measurements about rotating propellers or within moving rotor blades started in the early 1970's shortly after the development of workable LV systems. Since the laser velocimeter signal realization is inherently random, the direct application of conditional sampling and ensemble averaging algorithms is not possible. This drawback was bypassed in the past by complicated and slow oscilloscope/camera recording and 'sampling' techniques^{1,7} or by strobing or gating the data acquisition system.^{8,9}

Significant progress was reported by Powell, and Strazisar, et al.^{10,11} in 1980. Instead of gating the LV signal and measuring only at one angular position, they recorded simultaneously the transit time (velocity) and the corresponding angular position (angle). Despite the fact that the authors did not show any measured turbulence intensity blade to blade distribution, the system is capable of measuring it, according to the remarks in Ref. 10.

Summarizing the literature survey, one can learn the following lessons:

- 1) No commercial system for direct conditional sampling of LV signal in the digital domain is available.
- 2) Application of LV to measurements within rotating propellers and rotors is extremely difficult and complicated.
- 3) Practically no measured blade to blade turbulence intensity distributions have currently been presented.
- 4) The need for these measurements is critical to the detailed understanding of the flow conditions around a rotating propeller or within a rotating rotor in order to improve their efficiency and performance.

The system developed by Powell et al.¹⁰ is capable of fulfilling most of the requirements. The system described in this paper and in Refs. 12-14 is more advanced in some respects. First, this system is capable of simultaneous measurement of two velocity components without directional ambiguity. Second, higher data rates and thus shorter total time of measurement can be achieved because of more efficient data processing. Third, this system is more flexible as

Presented as Paper 83-1354 at the AIAA/SAE/ASME 19th Joint Propulsion Conference, Seattle, Wash., June 27-29, 1983; received July 15, 1983; revision received Oct. 18, 1983. Copyright © American Institute of Aeronautics and Astronautics, Inc., 1983. All rights reserved.

*Scientist, Member AIAA.

†Specialist Engineer, Member AIAA.

far as circumferential resolution is concerned. Fourth, time histories or blade to blade distributions are routinely produced not only for both velocity components, but also for both turbulence intensity components and even for Reynolds stresses between both measured velocities.

Conditional Sampling with Laser Velocimeter

LV data is obtained only when a signal of a tracing particle crossing the measurement volume is properly validated by the LV signal processor. The randomness of the laser velocimeter signal prevents the direct application of the commonly used techniques for conditional sampling to acquire ensemble averaged blade to blade velocity and turbulence intensity distributions. Since direct conditional sampling algorithms are inapplicable, a modified procedure has been developed.^{12,14}

Triggering pulses synchronized with the propeller speed initiate acquisition of the LV data as schematically shown in Fig. 1. The minimum time between successive LV data for both velocity components is $8 \mu\text{s}$ at present. During data reduction, the software procedure divides the time of one propeller revolution into a given number of equally spaced time slots, 360 in this particular case. Because this procedure is independent of the data acquisition procedure, the data acquisition speed is not decreased at all. Furthermore, the number of time slots, which determines the circumferential resolution, can be readily changed during postprocessing. Based on the time between samples, which is recorded during

data acquisition, a LV data point is assigned to the time slot that best approximates the actual time from the triggering pulse.

The data reduction procedure takes data over all intervals and assigns all LV data points in corresponding time slots of the single resulting file. A mean value of a velocity per individual time slot is then computed and this value is allocated to the center of each of the time slots, as indicated in Fig. 2. This ensemble average gives the desired velocity time history over one propeller revolution.

The data allocated to the individual time slots are treated as independent data sets assigned to the time at the center of the corresponding slot. A root mean square value of the set with respect to its mean value is a measure of the local turbulence intensity at a given angular position between blades.

A number of LV data points in each of the time slots of the resulting file is also registered. This is very important especially for measurement within the propeller disk, because the data points distribution helps to properly identify the flow regions shadowed by the blade and thus invisible to the LV. This distribution also gives an idea about the concentration of seeding particles in different regions of the flowfield.

Test Facility

The tested propeller was a two bladed, 330.2 mm diam wooden model airplane propeller TF13.6. The propeller was tested only at one speed $n=4250$ rpm. The corresponding

Fig. 1 Data acquisition scheme

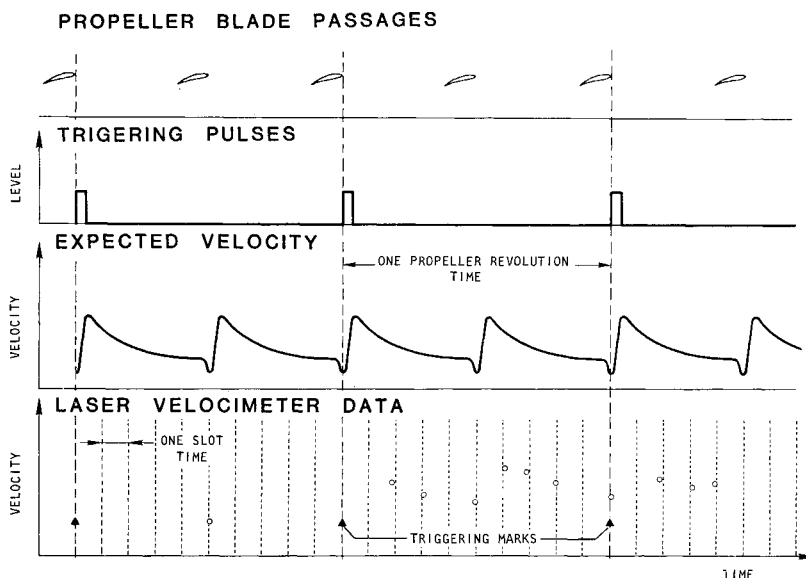
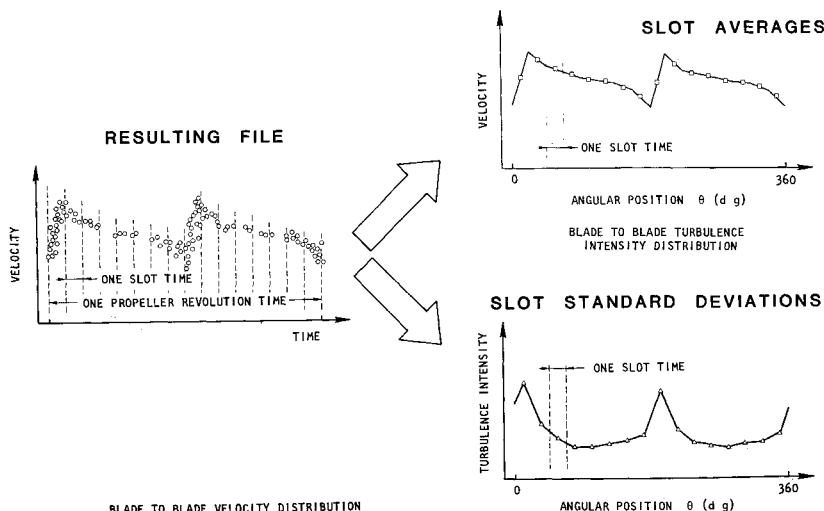


Fig. 2 Data reduction scheme



blade tip velocity and average blade tip Mach number were $U_{BT} = 73.5$ m/s and $M_{BT} = 0.215$, respectively

Front view and planview drawings of the test stand and LV arrangement are in Fig 3. The propeller was driven by a pneumatic motor which was connected with a flexible shaft. The bearing house of the propeller was mounted on a positioning table, enabling alignment of the propeller coordinate system with the LV coordinate system.

The laser velocimeter was arranged in a forward scatter mode with collecting optics placed 30 deg off axis.

The effective length of the measurement volume was 1 mm and diameter was 0.15 mm. The total power of both colors at the measurement volume was 1.1 W. The velocimeter used frequency shifting by a Bragg cell for both velocity components to avoid a velocity ambiguity.

A commercial insect fogger was used as a particle generator by burning oil fog injected into the heater. The average particle diameter was $0.9 \mu\text{m}$. The corresponding Stokes number was 0.0075, which was below the required minimum value of 0.01 for maximum speed error less than 1%, and maximum angle error less than 1 deg.¹⁵ The data rate for each of the velocity components reached up to 3000 validated data points per second.

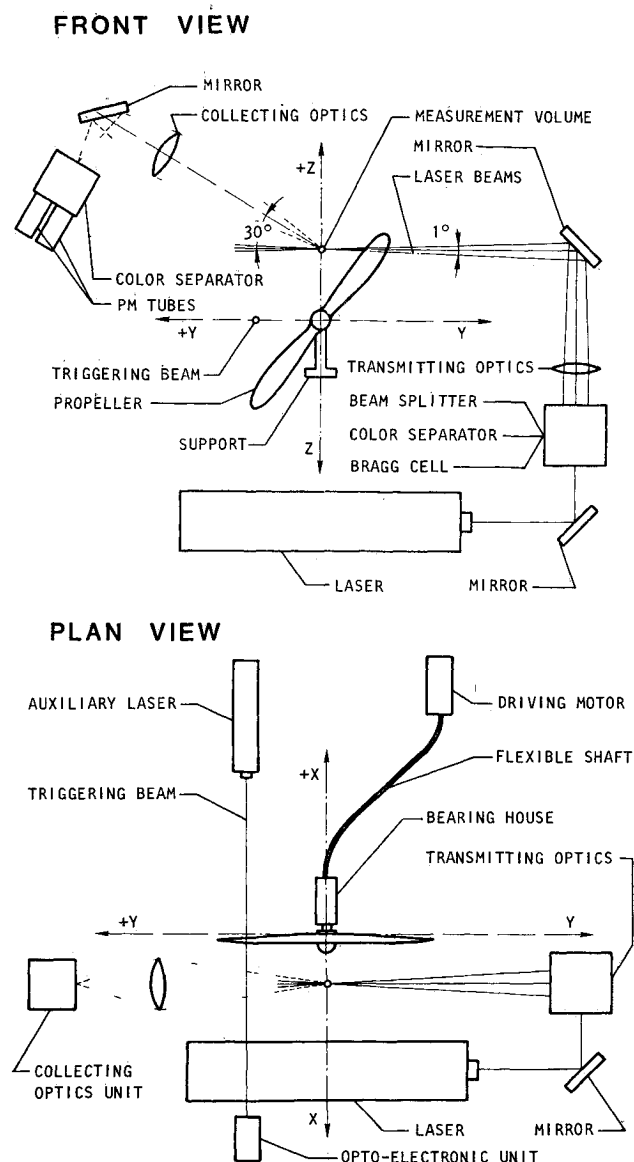


Fig 3 Test stand and LV arrangement

Experimental Results

Time Averaged (Mean) Distributions

The program consisted of acquiring mean velocity and turbulence intensity data for all three velocity vectors. Lockheed's laser velocimeter enables simultaneous measurement of only two velocity components at present, thus requiring two sets of measurements to acquire all three components.

Mean Velocities

The experimental results of the mean velocity measurements for all three components are presented in Figs 4 and 5. The axial distributions were measured at dimensionless radius 0.693 and radial profiles were measured just in front of the propeller and behind it.

Mean Turbulence Intensities

The distributions of all three mean turbulence intensity components were measured at identical locations as mean velocities and are plotted in Figs 6 and 7. Turbulence intensity is expressed in percentage and is computed as a root mean square standard deviation of local velocity fluctuations normalized by blade tip velocity U_{BT} .

Ensemble Averaged (Blade to Blade) Distributions

Ensemble averaged distributions yield the blade-to-blade distributions of components of local velocity and turbulence intensity along the circumference at a given radius and a given axial location. For a circumferential resolution of 1 deg, the acquisition of about 36,000 data inputs is needed to maintain an average of 100 data inputs per time slot.

The mean velocities and mean turbulence intensities were computed from blade-to-blade distributions as average values over the time corresponding to one propeller revolution. These computed values, given in Figs 8 and 9, were compared with measured mean values when the conditional sampling procedure was not employed (Figs 4-7). Both methods gave practically identical results as far as mean values are concerned.

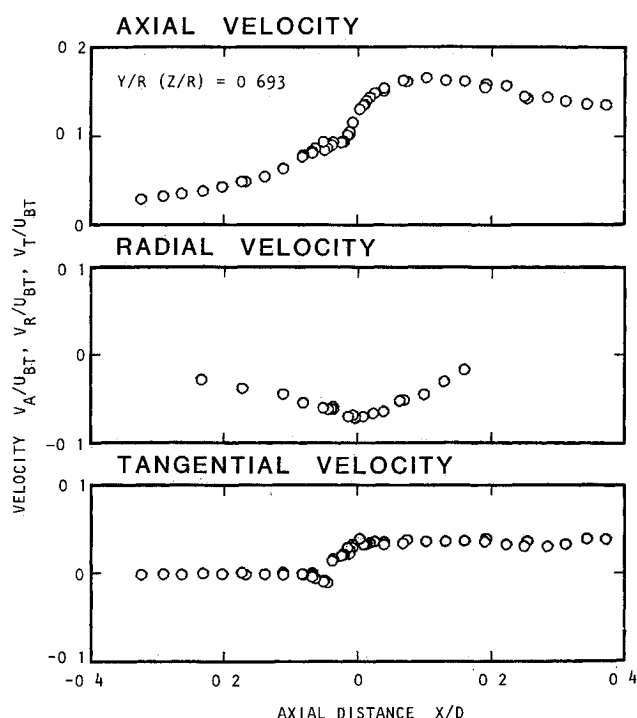


Fig 4 Axial variation of mean velocity components

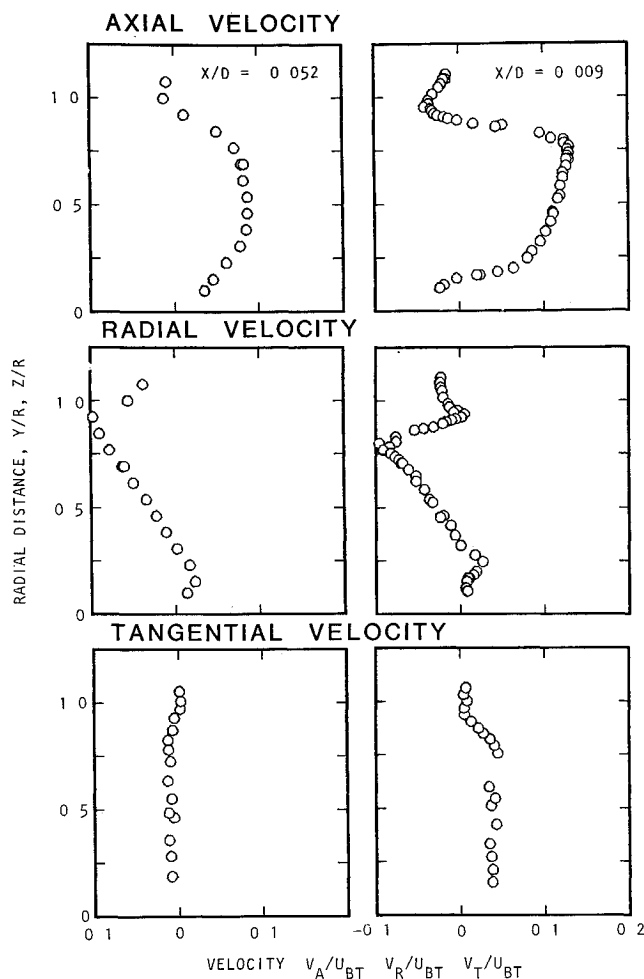


Fig 5 Radial profiles of mean velocity components

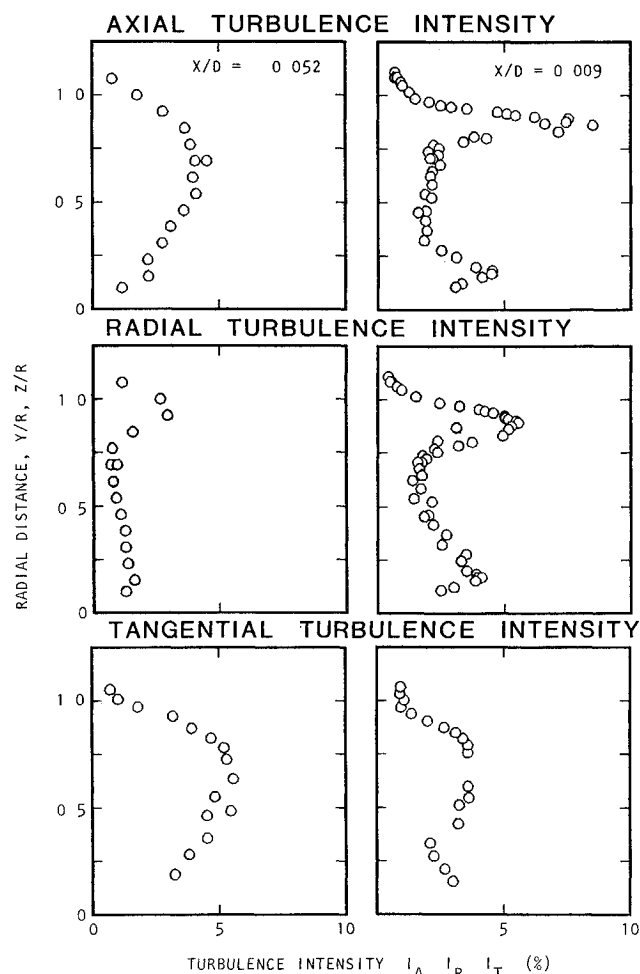


Fig 7 Radial profiles of mean turbulence intensity components

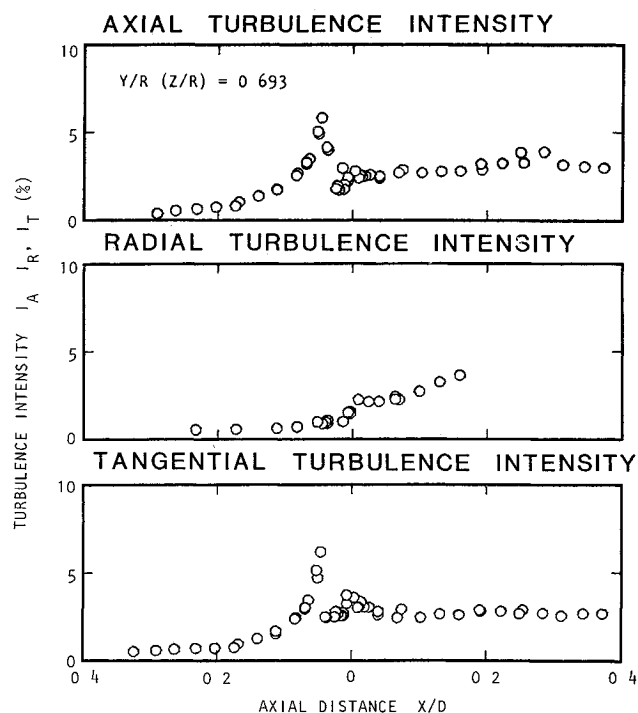


Fig 6 Axial variation of mean turbulence intensity components

Velocity Distributions

The blade to blade distributions of the axial and tangential velocity components are plotted in Fig 8. The measurements were done at $Y/R = -0.693$, which is in the region where the axial component of a mean velocity reaches its maximum in the near field behind the propeller.

Turbulence Intensity Distributions

Blade to blade distributions of turbulence intensity were measured simultaneously with the velocity distributions. The axial and tangential components of turbulence intensity measured at different axial locations at radial position $Y/R = -0.693$ are plotted in Fig 9.

Data Analysis and Interpretation

Mean Velocity Analysis

Inspection of the measured mean velocities and turbulence intensities reveals the complexity of the flowfield of a static propeller. Data show that a large part of the propeller disk experiences a reverse flow. The regions of an intensive flow separation and reverse flows are clearly visible in vector plots in Fig 10.

Axial Velocity Component

Axial distribution in Fig 4 shows the continuous increase of the induced velocity with an increasing axial distance. At a dimensionless radius of 0.693 the axial velocity component reaches its maximum at approximately $X/D = 0.1$ and then starts to gradually decrease.

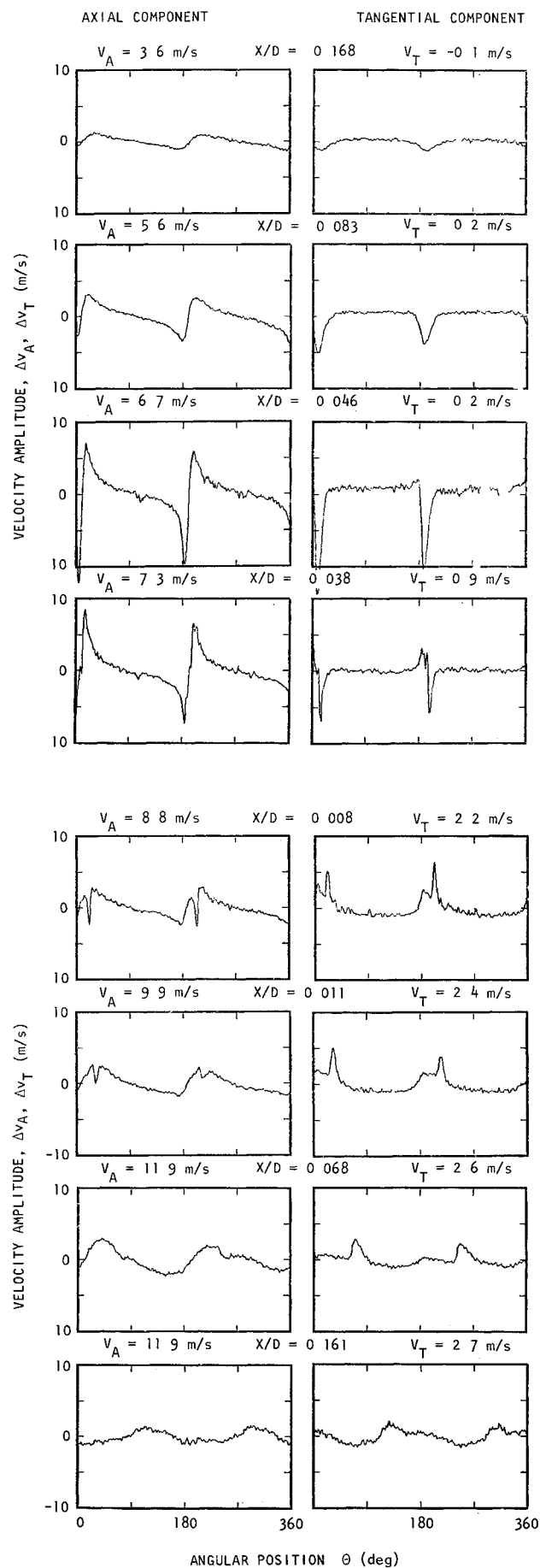


Fig 8 Time histories of axial and tangential velocity components ($Y/R = -0.693$, $Z/R = 0$)

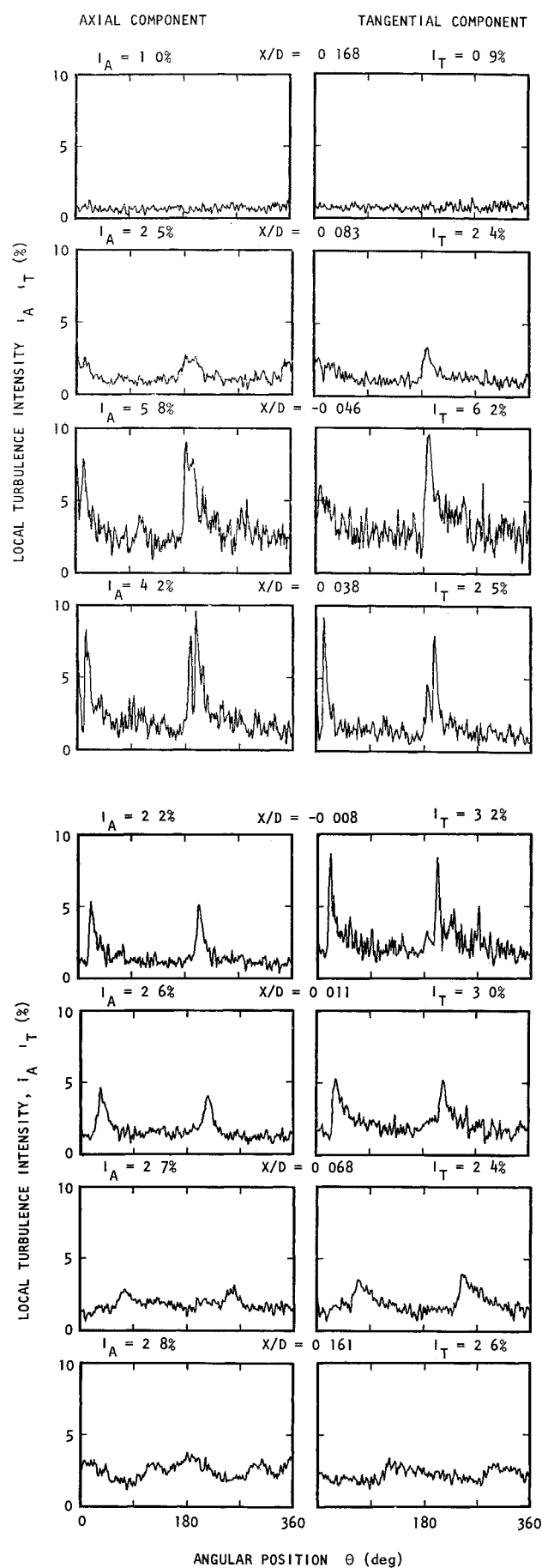
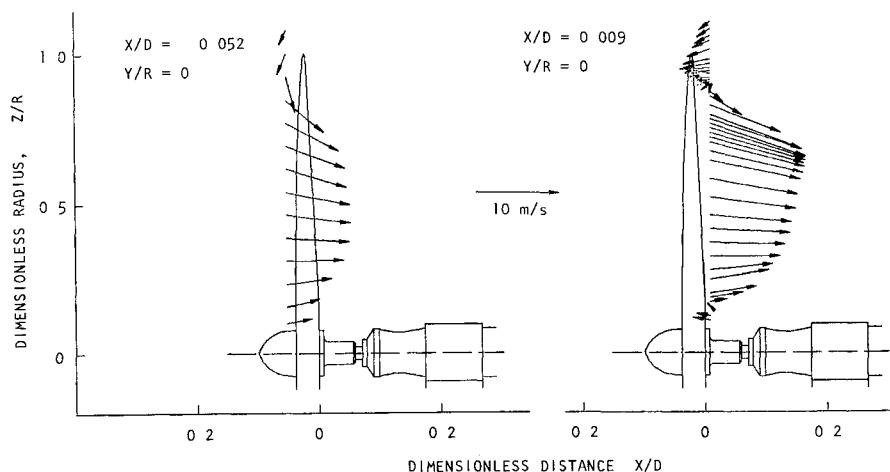


Fig 9 Time histories of local axial and tangential turbulence intensities ($Y/R = -0.693$, $Z/R = 0$)

Fig 10 Flow patterns in axial radial plane



Radial Velocity Component

The radial velocity component (Figs 4 and 5) reaches its largest magnitude in the negative direction in the region of the flow separation at the blade tip close to the propeller disk. It experiences very sharp changes in gradient in the radial direction. These changes stress the three dimensional character of the flow in this region. However the radial component recovers relatively rapidly towards small magnitude with increasing distance from the propeller disk. This recovery seems to be faster behind the propeller disk than in front of it. The radial component remains negative nearly everywhere in the propeller flow indicating the slipstream contraction.

Tangential Velocity Component (Flow Angle)

Tangential velocity which in fact defines the swirl of the slipstream is close to zero in front of the propeller disk as expected and reaches some constant value behind the propeller. However, a closer look in Fig 4 reveals that in the very narrow region just in front of the propeller disk, before the tangential component starts to rise it turns at first to the negative values. The radial profiles in Fig 5 confirm it also. Mean flow angle axial distribution at dimensionless radius 0.693 is plotted in Fig 11. The diagram clearly shows the negative prewhirl of the mean flow just before entering the propeller disk.

Radial distributions of the mean relative flow angle β just in front of the propeller disk and behind it are plotted in Fig 12 together with the blade pitch angle ϕ . The angle of the relative flow leaving the propeller disk agrees very well with the blade pitch angle ϕ in the middle part of the propeller disk while it differs significantly in the regions of the separated flow. Finally, in Fig 12 there is also depicted a radial distribution of the angle of attack i . The diagram shows moderate values of the angle of attack in the region of blade attached flow but rapidly increasing values of the angle of attack toward the hub or propeller blade tip. This rapid increase of the angle of attack ultimately leads to the flow separation from the blade.

Mean Turbulence Intensity Analysis

Axial Turbulence Intensity Component

The axial distribution of the axial turbulence intensity at dimensionless radius 0.693, plotted in Fig 6 shows a sharp and high turbulence intensity peak reaching 6% just ahead of the propeller disk. There is a sudden drop in turbulence intensity behind the propeller disk and then the turbulence intensity remains at $\sim 2.5\%$ far beyond the propeller.

Radial Turbulence Intensity Component

The radial turbulence intensity in the region of the attached flow increases immediately after the fluid passage through the

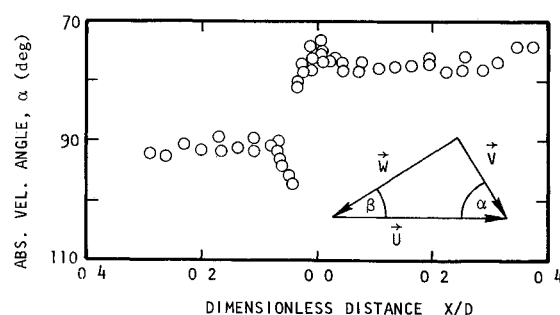


Fig 11 Axial distribution of absolute velocity angle

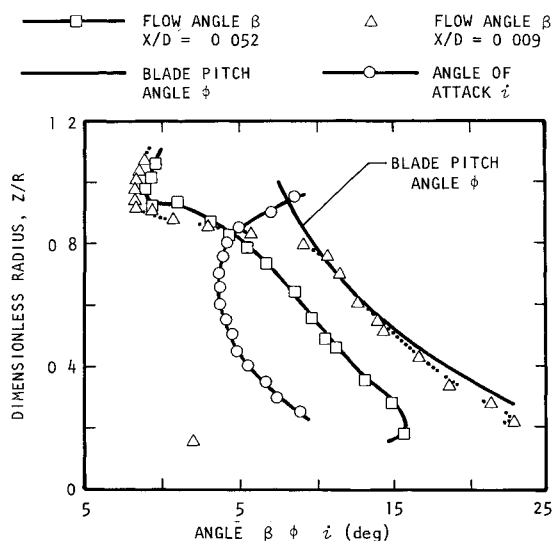


Fig 12 Radial distributions of relative velocity angles, blade pitch angle, and angle of attack

propeller disk and then remains more or less constant up to $X/D=0.2$ as seen in Fig 6. The increase of the radial turbulence observed beyond $X/D=0.1$ is due to the shifting of the high turbulent flow associated with the blade tip separation towards the centerline with an increasing axial distance. The axial decay of the maximum level of radial turbulence intensity is slower than the corresponding decay of the axial turbulence intensity component, as seen in Fig 13.

Tangential Turbulence Intensity Component

The axial distribution of the tangential turbulence intensity resembles that of the axial turbulence component (Fig 6).

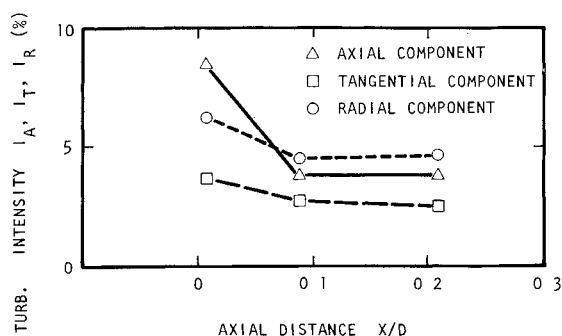


Fig 13 Axial variation of maximum turbulence intensity

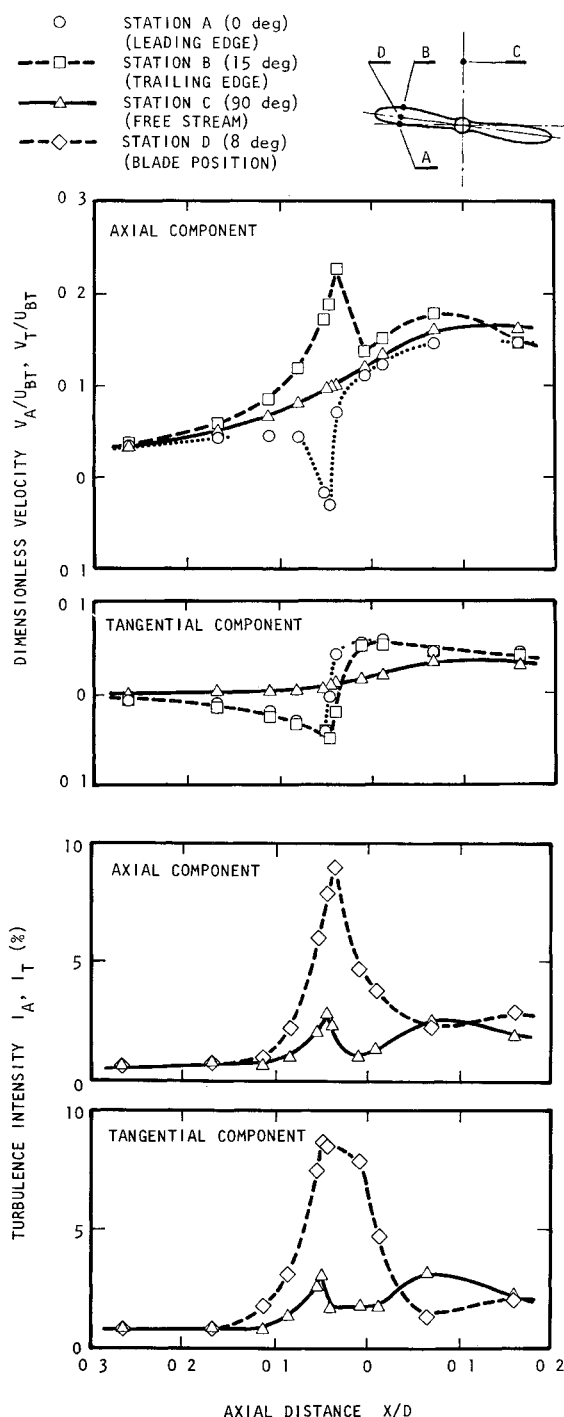


Fig 14 Axial variation of local velocities and local turbulence intensities

Again a very sharp peak is seen just ahead of the propeller disk followed by a sudden drop in the turbulence level. In this case however there is a second peak in the tangential turbulence intensity distribution located just behind the propeller. The level of the tangential component of turbulence intensity in the region of attached flow is higher than the levels of the other two turbulence intensity components. Also the decrease of turbulence intensity with an increasing axial distance is more gradual as seen in Fig 13.

Blade to Blade Velocity Distributions

The blade to blade distributions confirm the results of mean velocity measurements but in addition they also show significant nonuniformity of the time history of measured parameters. Velocity variations along three angular stations fixed with respect to the rotating propeller were analyzed. The first angular station was chosen to be at the blade leading edge marked A as shown in the insert in Fig 14, the second one at the blade trailing edge marked B and the third one marked C was located between the blades. As seen in Fig 14 there is a significant difference in the axial velocity development along these three angular stations. In the region between blades at station C the axial velocity smoothly increases in the broad vicinity of the propeller disk. The axial velocities at the other two stations experience severe acceleration and deceleration in the region of the propeller disk. The fluid velocity decelerates rapidly and even reverses at the propeller leading edge (station A) and then in the propeller disk is immediately accelerated to the velocity level of the freestream. At the propeller trailing edge (station B) the axial velocity is first gradually accelerated to the velocity level 2.5 times higher than the corresponding velocity in the freestream and then very rapidly decelerates to the freestream velocity level after the passage through the propeller disk.

The tangential velocity is zero in the freestream region (station C) in front of the propeller and gradually rises in the direction of the blade rotation to a positive level behind the propeller. In the blade region at the leading and trailing edges (stations A and B) the tangential velocity rises to negative values approaching the propeller disk which means that fluid flows in the direction opposite to the blade motion. In the propeller disk and immediately behind it the fluid velocity is rapidly accelerated by blade and wake impact in the direction of the blade rotation. Behind the propeller the tangential velocity at stations A and B gradually decreases to the freestream tangential velocity level.

Based on the inspection of the plots in Fig 14 it has become clear that the negative prewhirl in front of the propeller is limited only to the narrow region close to the blade and rotates with the blade. However in this region the flow angle reaches very high negative values while in the rest of the flowfield in the circumferential direction the flow angle keeps small positive values.

Blade to Blade Turbulence Distributions

The axial distributions of the axial turbulence intensity between the propeller blades in the freestream (station C) and in the blade region (station D) are also plotted in Fig 14. The figure shows a very sharp peak of the axial turbulence intensity close to the blade in the propeller disk region. A visible turbulence increase is also in the freestream region in the propeller disk. Immediately behind the propeller disk the turbulence intensity drops.

As far as tangential turbulence intensity component is concerned there is a broader region of a high turbulence intensity behind the propeller disk at the blade (station D) due to the effect of the intense blade wake on the flow turbulence. The freestream tangential turbulence component resembles the similar distribution of the axial component of the turbulence intensity.

Conclusion

A data reduction ensemble averaging technique employing laser velocimetry has been developed and verified. The mean velocity and mean turbulence intensity values computed from the ensemble averaged distributions were identical to directly measured mean values of velocity and turbulence intensity. The presented results have confirmed the ability of Lockheed's LV to conduct efficient measurements in a three dimensional complex flowfield about a rotating propeller. This technique is capable of revealing fine details of the nonstationary velocity flowfield of a rotating propeller. These details are very important for full understanding of the propeller aerodynamics and noise generation.

Besides the verification of the new data acquisition and reduction procedures, information about a flowfield of a rotating propeller was also acquired. Separated and reverse flow regions were localized on a rotating static propeller. The radial distribution of the propeller section angle of attack was measured while the propeller was in motion. The axial distribution of swirl angle revealed the existence of a negative prewhirl just in front of the propeller disk. This negative prewhirl is limited only to the narrow region close to the blade, and rotates with the blade.

The phenomena revealed by this series of measurements have stressed the necessity to investigate the characteristics of drastic changes in velocity and turbulence intensity close to the propeller in terms of their influence on the noise generation mechanism. The laser velocimeter has been shown to be a very powerful tool for experimental investigations of this nature.

Acknowledgments

This work was conducted under Lockheed Georgia IRAD funding. The authors are grateful to Dr. H. K. Tanna and D. M. Smith for their support and encouragement throughout the course of this work. Technical help from W. E. Carter is also particularly acknowledged.

References

- ¹Wisler, D. C. and Mossey, P. W. 'Gas Velocity Measurements Within a Compressor Rotor Passage Using the Laser Doppler Velocimeter', *AMSE Journal of Engineering for Power*, Vol. 95, April 1973, pp. 91-96.
- ²Sullivan, J. P. 'An Experimental Investigation of Vortex Rings and Helicopter Rotor Wakes Using a Laser Doppler Velocimeter',

Massachusetts Institute of Technology, Aerophysics Laboratory, Cambridge, Mass., TR183, June 1973.

³Orioff, K. L., Corsiglia, V. R., Biggers, J. C. and Ekstedt, T. W. 'Investigating Complex Aerodynamic Flows with a Laser Velocimeter', 'The Accuracy of Flow Measurements by Laser Doppler Methods', *Proceedings of the LDA Symposium*, Copenhagen, Denmark, Aug. 1975, pp. 624-643.

⁴Wisler, D. C. 'Shock Wave and Flow Velocity Measurements in a High Speed Fan Rotor Using the Laser Velocimeter', *AMSE Journal of Engineering for Power*, Vol. 99, April 1977, pp. 181-188.

⁵Sullivan, J. P. 'LDV Measurements on Propellers, Laser Velocimetry and Particle Sizing', *Proceedings of the Third International Workshop on Laser Velocimetry*, Purdue University, Lafayette, Ind., July 1978, pp. 531-534.

⁶Laser Optical Measurement Methods for Aero Engine Research and Development', AGARD Lecture Series AGARD LS 90, 1977.

⁷Landgrebe, A. J. and Johnson, B. V. 'Measurement of Model Helicopter Rotor Flow Velocities With a Laser Doppler Velocimeter', *Journal of the American Helicopter Society*, Vol. 19, July 1974, pp. 39-43.

⁸Runstadler, P. W. Jr. and Dolan, F. X. 'Design, Development and Test of Laser Velocimeter for High Speed Turbomachinery', *The Accuracy of Flow Measurements by Laser Doppler Methods, Proceedings of the LDA Symposium*, Copenhagen, Denmark, Aug. 1975, pp. 523-552.

⁹Walker, A. D., Williams, M. C. and House, R. D. 'Intrablade Velocity Measurements in a Transonic Fan Utilizing a Laser Doppler Velocimeter', *Minnesota Symposium on Laser Anemometry*, University of Minnesota, Oct. 1975, pp. 124-145.

¹⁰Powell, J. A., Strazisar, A. J., and Seasholtz, R. G. 'Efficient Laser Anemometer for Intra Rotor Flow Mapping in Turbomachinery', *AMSE Journal of Engineering for Power*, Vol. 103, April 1981, pp. 424-429.

¹¹Strazisar, A. J. and Powell, J. A. 'Laser Anemometer Measurements in a Transonic Axial Flow Compressor Rotor', *AMSE Journal of Engineering for Power*, Vol. 103, April 1981, pp. 430-437.

¹²Lepicovsky, J., Bell, W. A. and Ahuja, K. K. 'Conditional Sampling with a Laser Velocimeter and its Application for Large Scale Turbulent Structure Measurement', Lockheed Georgia Company, Marietta, Ga., Rept. LG83ER0007, Jan. 1983.

¹³Bell, W. A. and Lepicovsky, J. 'Conditional Sampling with a Laser Velocimeter', AIAA Paper 83-0756, April 1983.

¹⁴Lepicovsky, J. and Bell, W. A. 'Aerodynamic Measurements About a Rotating Propeller with a Laser Velocimeter with Conditional Sampling', Lockheed Georgia Company, Marietta, Ga., Rept. LG83ER0008, Jan. 1983.

¹⁵Dring, R. P. 'Sizing Criteria for Laser Anemometry Particles', *ASME Journal of Fluids Engineering*, Vol. 104, March 1982, pp. 15-17.